Excitonic two-photon absorption in carbon nanotubes

Seiji Uryu[A], Hiroshi Ajiki[B], and Tsuneya Ando[A]

Department of Physics, Tokyo Institute of Technology[A]
Department of Materials Engineering Science, Osaka University[B]

We theoretically study excitonic two-photon absorption in semiconducting carbon nanotubes within an effective-mass approximation. Sharp absorption peaks appear at energies of the second and fourth lowest exciton states below the interband continuum. The results are in good agreement with recent experiments.

I. INTRODUCTION

Carbon nanotubes, which are rolled-up two-dimensional (2D) graphite sheets, exhibit strong exciton effects, mainly revealed by one-photon absorption. Two-photon absorption gives complementary information on excited excitons which are inaccessible by one-photon absorption. In this paper, we shall briefly review our recent theoretical study on the two-photon absorption spectrum of semiconducting carbon nanotubes within an effective-mass approximation including exciton effects [1].

It was theoretically predicted that the Coulomb interaction prominently affects optical absorption in semiconducting carbon nanotubes [2, 3]. The band gap is considerably enhanced and exciton binding energy is comparable to but slightly smaller than this enhancement. As a result, the intensity is focused on exciton energy levels in linear absorption spectra. This prediction was later confirmed both theoretically [4–9] and experimentally [10–13].

Two-photon absorption has also been studied [14–21]. Photoluminescence experiments with two-photon absorption revealed that difference between the energies of one- and two-photon transitions is substantial, typically a few hundred meV, leading to the clear conclusion that the absorptions arise from excitons [18–20]. Moreover, calculations with exciton effects were performed and used for the estimation of exciton binding-energy from experimental one- and two-photon peaks.

II. MODEL AND METHOD

In a 2D graphite sheet shown in Fig. 1(a), the conduction and valence bands consisting of π states cross at K and K' points and the electron motion around these points is described well by a $\mathbf{k}\cdot\mathbf{p}$ equation corresponding to a relativistic Dirac equation with vanishing rest mass. Around the K point, for example, it is given by [22–24]

$$\gamma(\vec{\sigma}\cdot\hat{\mathbf{k}})\mathbf{F}(\mathbf{r}) = \varepsilon\mathbf{F}(\mathbf{r}), \tag{1}$$

where $\mathbf{F}(\mathbf{r})$ is a two-component envelope function, the x and y coordinates are chosen in the circumference and the axis direction, respectively, as shown in Fig. 1(b), ε is an eigen energy, γ a band parameter, $\vec{\sigma} = (\sigma_x, \sigma_y)$ the Pauli spin matrix, and $\hat{\mathbf{k}} \equiv -i\vec{\nabla}$ a wave vector operator.

Electronic states for a nanotube with a sufficiently large diameter are obtained by imposing the boundary condition around the circumference direction:

$$\mathbf{F}(\mathbf{r}+\mathbf{L}) = \mathbf{F}(\mathbf{r})\exp\Big(-\frac{2\pi i\nu}{3}\Big), \tag{2}$$

with $\mathbf{L}$ being a chiral vector shown in Fig. 1(a) and ν an integer determined uniquely as $\nu = 0$ or ±1 through $n_a + n_b = 3M + \nu$ with integer M, where n_a and n_b are integers defined by $\mathbf{L} = n_a\mathbf{a} + n_b\mathbf{b}$ and $\mathbf{a}$ and $\mathbf{b}$ are the primitive translation vectors shown in Fig. 1(a). The energy bands become

$$\varepsilon_{\pm,n}(k) = \pm\gamma\sqrt{\kappa_\nu(n)^2 + k^2}, \tag{3}$$

where $+$ and $-$ denote the conduction and valence band, respectively, k is a wave vector in the axis direction, and

$$\kappa_\nu(n) = \frac{2\pi}{L}\Big(n - \frac{\nu}{3}\Big), \tag{4}$$

with integer n and $L = |\mathbf{L}|$. Around the K' point the $\mathbf{k}\cdot\mathbf{p}$ equation is given by Eq. (1) where $\vec{\sigma}$ is replaced by complex conjugate $\vec{\sigma}^*$. The boundary condition becomes Eq. (2) with replacement $\nu \to -\nu$.

A screened Hartree-Fock approximation is used for interaction effect on the band structure and an attractive electron-hole interaction is introduced by using the Coulomb interaction screened by a static dielectric function [2, 3]. This approximation was shown to be sufficient by calculations in which dynamical effects are fully included [25, 26].

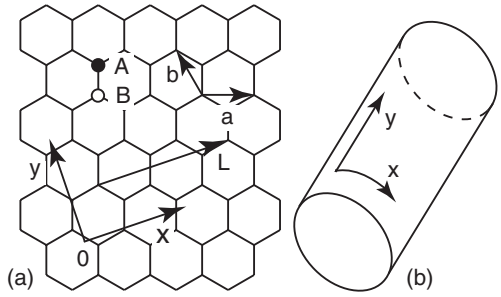

FIG. 1: Schematic illustration of (a) 2D graphite and (b) nanotube.

An exciton with the zero momentum is written as

$$|u\rangle = \sum_n \sum_k \psi_n^u(k) c_{+,n,k}^\dagger c_{-,n,k} |g\rangle, \qquad (5)$$

where $c_{+,n,k}^\dagger$ and $c_{-,n,k}$ are the creation and annihilation operators, respectively, with $\pm$ indicating the conduction and valence bands and $|g\rangle$ is the ground state. Solving an equation of motion [2, 3], $\psi_n^u(k)$ and exciton energy ε_u are obtained. The wave function $\psi_n^u(k)$ is an even or odd function of k, that is,

$$\psi_n^u(-k) = \pm \psi_n^u(k). \qquad (6)$$

In the following, we shall confine ourselves to the low-energy regime below the interband continuum and therefore completely neglect multi-exciton states such as bi-exciton. For parallel polarization where the electric field is given by

$$E_x = 0, \quad E_y = E(e^{-i\omega t} + e^{i\omega t}), \qquad (7)$$

a two-photon energy-absorption rate per unit length is given by $\beta(\omega)E^4$ with an absorption coefficient

$$\beta(\omega) = \frac{4\pi e^4}{\omega^3 A} \sum_{K,K'} \sum_u \left| \sum_{u'} \frac{\langle u|\hat{v}_y|u'\rangle\langle u'|\hat{v}_y|g\rangle}{\hbar\omega - \varepsilon_{u'}} \right|^2 \times \delta(2\hbar\omega - \varepsilon_u), \qquad (8)$$

where $\hat{v}_y$ is a velocity operator in the axis direction. Using typical scales of physical quantities in nanotubes, a dimensionless absorption coefficient $\bar{\beta}(\omega)$ is given by

$$\beta(\omega) = \frac{e^4 L^5}{8\pi^3 \hbar \gamma^2} \bar{\beta}(\omega). \qquad (9)$$

Then, we can see that the absorption coefficient is proportional to the fifth power of the circumference length.

The velocity matrix elements for the K point are given by

$$\langle u'|\hat{v}_y|g\rangle = \frac{i\gamma}{\hbar} \sum_n \sum_k \frac{\kappa_\nu(n)}{\sqrt{\kappa_\nu(n)^2 + k^2}} \psi_n^{u'}(k)^*, \qquad (10)$$

and

$$\langle u|\hat{v}_y|u'\rangle = -\frac{2\gamma}{\hbar} \sum_n \sum_k \frac{k}{\sqrt{\kappa_\nu(n)^2 + k^2}} \times \psi_n^u(k)^* \psi_n^{u'}(k). \qquad (11)$$

Those for the K' point are given by the complex conjugate of the above with the replacement $\nu \to -\nu$. It can be seen from Eqs. (10) and (11) that states with even parity are excited from the ground state by one-photon absorption and those with odd parity are excited by two-photon absorption.

The strength of the Coulomb interaction is characterized by dimensionless parameter $(e^2/\kappa L)(2\pi\gamma/L)^{-1}$, which is the ratio of the typical Coulomb energy $e^2/\kappa L$ and the typical kinetic energy $2\pi\gamma/L$, where κ is an effective dielectric constant. The band parameter is related to hopping integral γ_0 through $\gamma = (\sqrt{3}/2)a\gamma_0$ with lattice constant $a = 2.46$ Å in a nearest-neighbor tight-binding model. For a rough estimate of the interaction strength, we can use this relation with $\gamma_0 \sim 3$ eV and then have $(e^2/\kappa L)(2\pi\gamma/L)^{-1} \sim 0.35/\kappa$. The dielectric constant κ describes effects of screening by electrons in σ bands, core states, and the π bands away from the K and K' points and by the surrounding material if any. Its exact value is not known, but we can expect that κ is not so much different from 2.4 in bulk graphite. Then, the interaction parameter lies roughly in the range 0.1∼0.2.

The infinitely extending energy bands in Eq. (3) should be cut off by an energy ε_c of the order of the half of the π-band width $3\gamma_0$. Therefore, $\varepsilon_c(2\pi\gamma/L)^{-1} \approx (\sqrt{3}/\pi)(L/a) = \sqrt{3}d/a$, with d being the diameter of the nanotube. Since excitation energy exhibits only weak dependence on the cutoff energy [3], we use a typical value $\varepsilon_c(2\pi\gamma/L)^{-1} = 10$ corresponding to diameter ~ 1.4 nm in the followings. The kinetic energy $2\pi\gamma/L$, used as energy units, is about 1 eV for tubes with typical diameter $d \sim 1.4$ nm.

III. NUMERICAL RESULTS

A typical example of energy dependence of two-photon absorption coefficient is shown in Fig. 2 for $(e^2/\kappa L)(2\pi\gamma/L)^{-1} = 0.2$ where

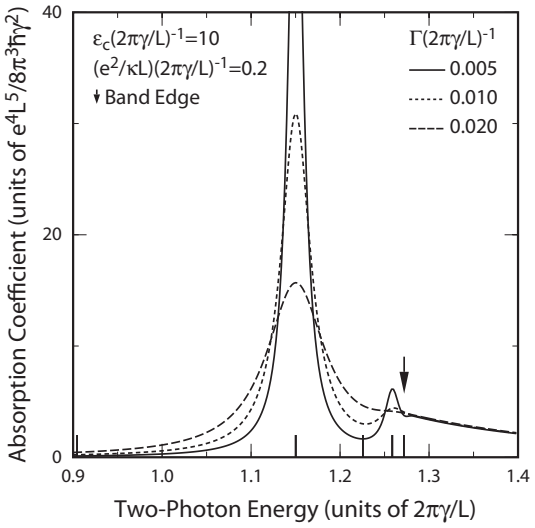

FIG. 2: Calculated two-photon absorption coefficient for $(e^2/\kappa L)(2\pi\gamma/L)^{-1} = 0.2$. Phenomenological broadening $\Gamma(2\pi\gamma/L)^{-1}$ is introduced. The arrows indicate the band edge and the short vertical lines at the bottom denote exciton energies.

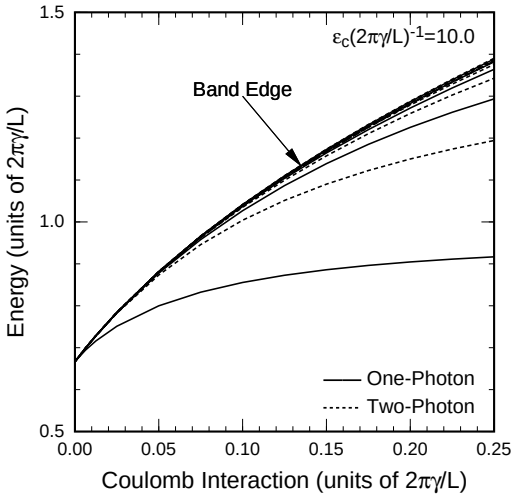

FIG. 3: Coulomb-interaction dependence of exciton energies associated with the lowest band. Solid and dotted lines denote excitons excited by one- and two-photon absorption, respectively.

energy broadening is introduced by using a Lorentzian function with a half width at half maximum Γ. The lowest band edge is shown by downward arrows. The energy of all the exciton bound states is indicated by short vertical lines at the bottom.

A prominent peak appears corresponding to the second lowest exciton with odd parity and

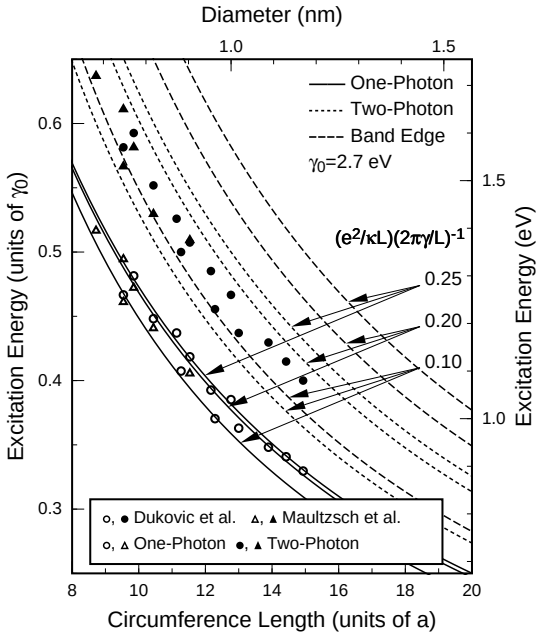

FIG. 4: Calculated excitation energies as a function of the circumference length. Solid and dotted lines denote the energies for one- and two-photon absorption, respectively, and dashed lines are the band edges. Symbols denote experimental results [19, 20] where open and closed symbols indicate one- and two-photon transitions, respectively.

another peak associated with the fourth lowest exciton appears. The difference between the first and second lowest exciton energies is approximately 0.22 in units of $2\pi\gamma/L$.

In Fig. 3, the Coulomb-interaction dependence of the exciton energies is shown. Solid and dotted lines denote excitons contributing to one- and two-photon absorption spectra, respectively. With increase of the interaction, many exciton bound states split off from the interband continuum. Similar results were previously reported for a different cutoff energy [2].

In Fig. 4, excitation energies are plotted as a function of the circumference length. Solid and dotted lines denote calculated energies of the two lowest excitons observable in one- and two-photon absorption, respectively, and dashed lines indicate band edges. Symbols are experimental results [19, 20] where open and filled symbols indicate excitons for one- and two-photon transitions, respectively. We have set $\gamma_0 \approx 2.7$ eV which was used for comparison with experiments for the lowest excitons associated with the first and second gaps in a previous paper [3].

As shown in Fig. 3, the energy of the low-

est exciton is weakly dependent on the interaction strength $(e^2/\kappa L)(2\pi\gamma/L)^{-1}$. Therefore, the band parameter is uniquely determined as approximately $\gamma_0 \approx 2.7$ eV. Using the position of the second exciton, strongly dependent on the Coulomb interaction, we can place the interaction parameter in the range $0.1 < (e^2/\kappa L)(2\pi\gamma/L)^{-1} < 0.2$. More precise determination becomes possible when we include other effects such as a higher order $\mathbf{k}\cdot\mathbf{p}$ term giving trigonal warping, curvature, and lattice distortions [3], leading to a family effect observed experimentally [12, 13].

IV. CONCLUSION

We have studied two-photon absorption spectra associated with excited exciton states of semiconducting carbon nanotubes for parallel polarization within the effective-mass approximation. Two-photon exciton peaks appear at energies of the second and fourth lowest levels with odd parity. The theory is in good agreement with experiments.

Acknowledgments

This work was supported in part by a 21st Century COE Program at Tokyo Tech "Nanometer-Scale Quantum Physics," Grants-in-Aid for Scientific Research, and Grant-in-Aid for Scientific Research on Priority Area "Carbon Nanotube Nanoelectronics" from the Ministry of Education, Culture, Sports, Science and Technology, Japan.

[1] S. Uryu, H. Ajiki, and T. Ando, Phys. Rev.B **78**, 115414 (2008).
[2] T. Ando, J. Phys. Soc. Jpn. **66**, 1066 (1997).
[3] T. Ando, J. Phys. Soc. Jpn. **73**, 3351 (2004).
[4] C. D. Spataru, S. Ismail-Beigi, L. X. Benedict, and S. G. Louie, Phys. Rev. Lett. **92**, 077402 (2004).
[5] C. D. Spataru, S. Ismail-Beigi, R. B. Capaz, and S. G. Louie, Phys. Rev. Lett. **95**, 247402 (2005).
[6] E. Chang, G. Bussi, A. Ruini, and E. Molinari, Phys. Rev. Lett. **92**, 196401 (2004).
[7] V. Perebeinos, J. Tersoff, and Ph. Avouris, Phys. Rev. Lett. **92**, 257402 (2004).
[8] H. Zhao and S. Mazumdar, Phys. Rev. Lett. **93**, 157402 (2004).
[9] C. L. Kane and E. J. Mele, Phys. Rev. Lett. **93**, 197402 (2004).
[10] M. Ichida, S. Mizuno, Y. Tani, Y. Saito, and A. Nakamura, J. Phys. Soc. Jpn. **68**, 3131 (1999).
[11] M. Ichida, S. Mizuno, Y. Saito, H. Kataura, Y. Achiba, and A. Nakamura, Phys. Rev. B **65**, 241407(R) (2002).
[12] M. J. O'Connell, S. M. Bachilo, C. B. Huffman, V. C. Moore, M. S. Strano, E. H. Haroz, K. L. Rialon, P. J. Boul, W. H. Noon, C. Kittrell, J. Ma, R. H. Hauge, R. B. Weisman, and R. E. Smalley, Science **297**, 593 (2002).
[13] S. M. Bachilo, M. S. Strano, C. Kittrell, R. H. Hauge, R. E. Smalley, and R. B. Weisman, Science **298**, 2361 (2002).
[14] Vl. A. Margulis and T. A. Sizikova, Physica B **245**, 173 (1998).
[15] Vl. A. Margulis and E. A. Gaiduk, J. Opt. A: Pure Appl. Opt. **3**, 267 (2001).
[16] E. J. Mele, P. Kral, and D. Tomanek, Phys. Rev. B **61**, 7669 (2000).
[17] W.-D. Cheng, D.-S. Wu, X.-D. Li, Y.-Z. Lan, H. Zhang, D.-G. Chen, Y.-J. Gong, Y.-C. Zhang, F.-F. Li, J. Shen, and Z.-G. Kan, Phys. Rev. B **70**, 155401 (2004).
[18] F. Wang, G. Dukovic, L. E. Brus, and T. F. Heinz, Science **308**, 838 (2005).
[19] J. Maultzsch, R. Pomraenke, S. Reich, E. Chang, D. Prezzi, A. Ruini, E. Molinari, M. S. Strano, C. Thomsen, and C. Lienau, Phys. Rev. B **72**, 241402(R) (2005).
[20] G. Dukovic, F. Wang, D. Song, M. Y. Sfeir, T. F. Heinz, and L. E. Brus, Nano Lett. **5**, 2314 (2005).
[21] H. Zhao, S. Mazumdar, C.-X. Sheng, M. Tong, and Z. V. Vardeny, Phys. Rev. B **73**, 075403 (2006).
[22] H. Ajiki and T. Ando, J. Phys. Soc. Jpn. **62**, 1255 (1993).
[23] T. Ando, J. Phys. Soc. Jpn. **74**, 777 (2005).
[24] J. C. Slonczewski and P. R. Weiss, Phys. Rev. **109**, 272 (1958).
[25] H. Sakai, H. Suzuura, and T. Ando, J. Phys. Soc. Jpn. **72**, 1698 (2003).
[26] H. Sakai, H. Suzuura, and T. Ando, Physica E **22**, 704 (2004).